

Guided Action Flow: Q-Guided Inference for Flow-Matching Vision-Language-Action Policies

Liuhaichen Yang¹, Zhuang Jiang¹, Chenchao Sheng¹, Zezhi Tang^{1*}

Abstract—Flow-matching vision-language-action policies generate robot action chunks through an iterative transport process, creating an opportunity for test-time guidance without retraining the base policy. We study this opportunity in Guided Action Flow, an inference-time framework that keeps a pretrained SmolVLA policy frozen and uses a learned action-chunk critic to guide its reverse-time flow sampler. The critic is trained from real success and failure rollouts, can condition on task-description features from the frozen SmolVLA language pathway, and is used only through action gradients during sampling. We evaluate the approach on LIBERO manipulation tasks. A single-task critic improves success from 68.0% to 82.0% on one seed window and from 82.0% to 86.0% on another. A multi-family task-description critic improves validation success from 46.0% to 56.0%, while the locked held-out test gain is positive but modest, from 65.0% to 67.5%. These results support the feasibility of Q-guided inference for frozen flow-matching VLA policies, while showing that critic generalization and uncertainty-aware guidance remain the central bottlenecks.

Index Terms—vision-language-action models, robot manipulation, flow matching, test-time guidance, offline reinforcement learning

I. INTRODUCTION

Vision-language-action (VLA) policies have become a practical route to language-conditioned robot manipulation. Earlier language-conditioned manipulation systems already showed that semantic task descriptions can improve generalization beyond fixed goal labels, using architectures that combine pre-trained vision-language features, imitation learning, or 3D action representations [1]–[3]. Recent VLA systems extend this direction by scaling policy learning with larger robot datasets, stronger language-vision backbones, and sequence-generation architectures. Systems such as RT-1, RT-2, PaLM-E, Open X-Embodiment, Octo, OpenVLA, π_0 , FAST, and SmolVLA scale policy learning by combining language conditioning, large robot datasets, and sequence-generation architectures [4]–[12]. This progress is especially relevant for benchmarks such as LIBERO, LIBERO-Plus, and LIBERO-PRO, which expose the difficulty of robust language-conditioned manipulation under task, object, layout, and evaluation distribution shifts [13]–[15]. Recent embodied interfaces, including SignVLA, further broaden the language and multimodal instruction channels through which robots may receive tasks [16].

The resulting policies are increasingly capable, but their adaptation story is still incomplete. A pretrained VLA may execute many benchmark tasks, yet still fail when the task

distribution shifts, when early actions create compounding errors, or when multiple plausible action chunks satisfy the language instruction locally but only one leads to task completion. The obvious response is to fine-tune the VLA. In practice, however, full-policy fine-tuning can be expensive, hardware-sensitive, and difficult to validate when the user only has a small amount of task-local data. This is especially true for consumer-GPU settings, which motivated the use of compact SmolVLA checkpoints in this project.

This paper studies a more modular adaptation path. Instead of updating the base policy, we train a smaller critic from rollouts of the frozen policy and use that critic only at inference time. The critic does not choose among a finite set of proposed actions, and it is not used to fine-tune the VLA. It provides a gradient over the continuous action chunk that biases the policy sampler toward higher-value actions. This design is attractive when the frozen policy is already competent enough to generate useful action candidates, but not reliable enough to solve every task instance.

Flow-matching and diffusion-style action policies make this idea especially natural. These policies produce actions through an iterative denoising or transport trajectory [10], [17]–[19]. In generative modeling, guidance methods modify intermediate samples using external gradients or conditional scores [20], [21]. In control, diffusion and flow policies have similarly been used for planning and policy improvement [22]–[25]. The closest conceptual prior is Q-Guided Flow (QGF), which studies test-time value-gradient guidance for flow policies in reinforcement learning [25]. Our goal is narrower and more empirical: we ask whether a QGF-style update can be made useful for a frozen flow-matching VLA policy, specifically SmolVLA on LIBERO tasks, using action-chunk critics trained from real rollouts.

This setting differs from standard offline RL in two ways. First, the action generator is not a policy trained from scratch for a fixed task family; it is a pretrained VLA with its own language-conditioned flow sampler. Second, the adaptation objective is deliberately minimal: preserve the base policy and only change the inference trajectory. This makes the method easy to attach to a frozen VLA, but also raises a sharp technical question: can a lightweight critic trained from sparse success and failure rollouts produce gradients that are helpful rather than harmful inside a high-dimensional action-chunk sampler?

We introduce Guided Action Flow, a local adaptation layer around frozen SmolVLA inference. During the SmolVLA reverse-time flow sampler, Guided Action Flow estimates the

¹ Department of Computer Science, University College London.
Correspondence: zezhi.tang@ucl.ac.uk

clean action chunk, differentiates a learned critic with respect to that chunk, clips and gates the resulting gradient, and updates the flow velocity before the sampler step. The base policy is never fine-tuned. Because the pinned SmolVLA implementation integrates from noise at $t = 1$ to actions at $t = 0$, the guidance sign must be derived from the actual sampler rather than copied from a forward-time flow formulation.

This paper is an early-stage empirical study rather than a broad generalization claim. The strongest result is not that QGF solves VLA adaptation; it is that critic gradients can improve a frozen SmolVLA policy in real LIBERO rollouts, and that task-conditioned critics with uncertainty-aware gating are the most promising path so far. The held-out improvements are positive but small, which points to critic generalization as the central open problem.

Our contributions are:

- We instantiate Q-guided test-time flow sampling for frozen VLA policies, deriving the correct guidance sign for the pinned reverse-time SmolVLA sampler.
- We design and train action-chunk critics from real LIBERO rollouts, including a task-description-conditioned variant using frozen SmolVLA VLM hidden-state features.
- We add uncertainty-aware guidance through a critic ensemble and disagreement gate, reducing guidance when critic predictions disagree.
- We report positive but bounded evidence on LIBERO: strong single-task gains, clear multi-family validation gains, and modest held-out improvement, alongside negative results for insufficiently general critics.

II. RELATED WORK

A. Vision-Language-Action Policies

Generalist robot policies build on earlier language-conditioned manipulation work. CLIPort combines semantic visual-language features with spatial manipulation primitives for tabletop tasks [1]. PerAct formulates multi-task manipulation as language-conditioned 6-DoF action prediction over voxel observations [2]. BC-Z studies zero-shot task generalization through scalable robotic imitation learning with language and video task conditioning [3]. These systems show the value of language as a task interface, but they are typically trained for narrower data regimes or policy architectures than recent VLA models.

Modern generalist robot policies increasingly use language and large-scale pretraining to improve transfer. RT-1 showed that transformer policies can scale with real robot data and language conditioning [4]. RT-2 moved further toward VLA modeling by co-training web-scale vision-language representations with robotic action prediction [5]. PaLM-E integrated continuous embodied observations into a multimodal language model, emphasizing the connection between general-purpose reasoning and embodied control [6]. Open X-Embodiment and RT-X standardized multi-robot datasets and models, making cross-embodiment training a concrete research direction [7].

Open policies have made this line of work easier to inspect and adapt. Octo is an open-source generalist policy trained on Open X-Embodiment data and designed for efficient fine-tuning across robots and sensory setups [8]. OpenVLA provides an open 7B-parameter VLA and studies efficient fine-tuning and serving [9]. SmolVLA targets affordable and efficient VLA training and deployment, making it a useful base policy for consumer-GPU adaptation studies [12]. FAST studies action tokenization for autoregressive VLA policies [11], while π_0 uses a flow-matching VLA architecture [10]. Guided Action Flow is complementary to these systems: it does not propose a new VLA backbone or action tokenizer, but adds an inference-time critic layer around a frozen flow-matching VLA.

Task-specific vision-based manipulation pipelines remain an important complementary direction, especially when object detection and grasp prediction can be engineered for a constrained domain [26]. Compared with such pipelines, VLA policies shift more task semantics into the language-conditioned policy itself. This makes frozen-policy adaptation useful: the system can preserve a general instruction-conditioned policy while adding task-local correction through the critic.

Instruction interfaces are also broadening. SignVLA studies sign-language-guided robotic manipulation, illustrating that embodied control may need to ground instructions from modalities beyond text [16]. This strengthens the motivation for modular adaptation layers: if task instructions and execution contexts vary, updating an entire VLA for every new interface or distribution may be unnecessarily costly.

B. Benchmarks for Robust Robotic Manipulation

LIBERO benchmarks knowledge transfer and lifelong robot learning across generated manipulation suites [13]. Its suites are useful for this study because they expose language-conditioned manipulation failures while remaining practical to run with open VLA checkpoints. LIBERO-Plus and LIBERO-PRO extend this direction by probing robustness under perturbations and memorization-sensitive evaluation protocols [14], [15]. These benchmarks are important because a high score on a standard task split may not imply robustness to camera, object, instruction, or initialization shifts. Our strongest current evidence is on vanilla LIBERO, while LIBERO-Plus and LIBERO-PRO serve as baseline anchors and planned expansion targets. We therefore avoid claims of robust benchmark-level transfer.

Robotic robustness is often addressed during training by exposing policies or perception modules to broader simulated variation. Domain randomization and dynamics randomization are representative strategies for narrowing the simulation-to-real gap by varying visual appearance or system dynamics before deployment [27], [28]. Guided Action Flow is complementary to this data-side view: it does not change the training distribution of the base VLA, but uses a rollout-trained critic to adjust the action-generation trajectory at test time.

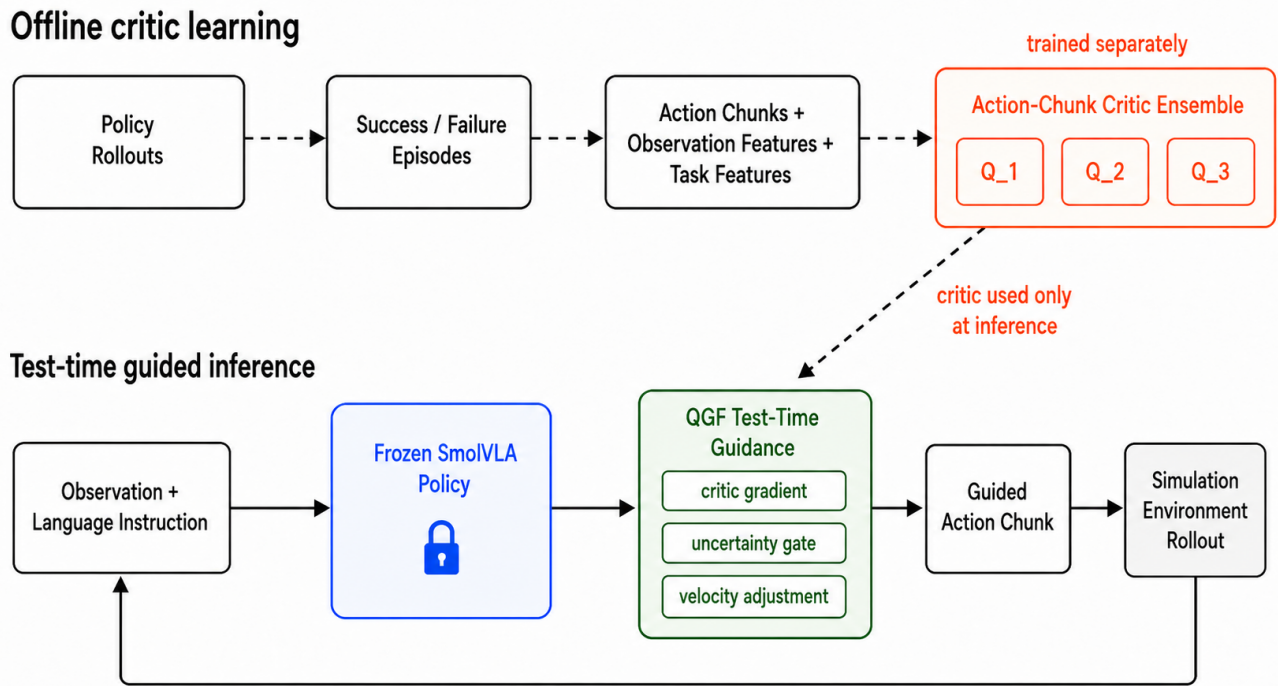


Fig. 1. System overview of Guided Action Flow. Offline rollouts from the frozen policy are converted into success/failure episodes and action-chunk training examples for a separately trained critic ensemble. At test time, SmolVLA remains frozen while QGF uses the critic ensemble through critic gradients, uncertainty gating, and velocity adjustment to guide action-chunk generation during closed-loop LIBERO evaluation.

C. Guidance for Generative Policies

Diffusion and flow models generate samples through iterative transformations from noise to data [17], [18]. Guidance modifies this trajectory using auxiliary information. Classifier guidance and classifier-free guidance are canonical examples in image generation [20], [21]. Their common theme is that a trained generator need not be retrained to change sampling behavior; a guidance signal can reshape the sampling path at inference time.

In robotics and reinforcement learning, Diffusion Policy shows that action diffusion can be an effective visuomotor policy class [19]. Diffuser plans by denoising trajectories and connects diffusion sampling with flexible decision-making [22]. Diffusion-QL and IDQL connect expressive diffusion policy classes with offline RL value learning [23], [24]. QGF directly studies test-time value-gradient guidance for flow policies [25]. Our work adapts this test-time guidance perspective to frozen VLA inference, where the action generator is a pretrained SmolVLA checkpoint, the action is a chunk produced by a VLA sampler, and the critic is trained from environment rollouts rather than from a standard offline RL benchmark dataset.

D. Robust Reinforcement Learning and Adaptive Control

Robust reinforcement learning provides another perspective on policy improvement under uncertainty. Prior work trains policies against model mismatch, adversarial disturbances, or

action perturbations through ensemble policy optimization, adversarial reinforcement learning, and action-robust objectives [29]–[31]. Adaptive dynamic programming, disturbance-observer control, and control-oriented robust RL study related questions in structured nonlinear systems, including robust output tracking for uncertain time-delay systems, tracking under process disturbances, disturbance-observer optimal tracking for slot-coating processes, RL-based stabilization with generalized disturbances, optimal tracking under mismatched disturbances, and event-triggered robust adaptive dynamic programming [32]–[38]. These methods usually optimize a policy or controller for a disturbance model, stability objective, or triggering rule. Broader industrial cyber-physical systems work also studies hierarchical testing and distributed constrained optimization for systems operating under coupled dynamics and inequality constraints [39], [40]. Guided Action Flow addresses a different regime: the plant-level controller is replaced by a pretrained language-conditioned flow policy, and the learned critic does not define a stabilizing controller. Instead, it supplies local action-chunk gradients inside a frozen VLA sampler. The connection is therefore conceptual rather than architectural: these lines of work all reflect the need for reliable behavior under uncertainty, but the representation, deployment interface, and failure modes differ substantially.

E. Offline Critics and Distribution Shift

Offline RL highlights the difficulty of learning value functions that are useful beyond the data distribution [41]. Con-

servative Q-Learning and Implicit Q-Learning address value overestimation and policy extraction under static datasets [42], [43]. Other approaches use model uncertainty penalties or Q-ensemble uncertainty to reduce out-of-distribution exploitation [44], [45]. These issues appear in our setting as well: a critic trained on limited task-family data can produce gradients that improve some episodes while harming others. The problem is amplified by action chunks. A small gradient error can alter a sequence of continuous actions, and that sequence is executed in a closed-loop environment where early mistakes change future observations. Our ensemble disagreement gate is a simple uncertainty-aware mitigation, not a complete solution to critic out-of-distribution behavior.

III. METHOD

A. Overview

Guided Action Flow is an inference-time wrapper around a frozen flow-matching VLA. It has three components. First, we collect rollouts from the frozen base policy in LIBERO and convert each episode into action-chunk training examples. Second, we train one or more critics that score candidate action chunks conditioned on observation and task features. Third, during SmolVLA sampling, we apply a value-gradient update to the flow velocity before each denoising integration step. The base denoising network and VLA language-vision backbone are not updated.

The method is deliberately not an action reranker. Reranking would sample several complete action chunks and pick one according to the critic. Instead, Guided Action Flow changes the continuous flow trajectory that produces the action chunk. This distinction matters because the critic can influence intermediate samples before the final action is produced, which is closer to the structure of diffusion and flow guidance.

B. Problem Setting

We consider a frozen VLA policy π_θ that maps a visual observation, robot proprioception, and language instruction to an action chunk $a_{0:H-1} \in \mathbb{R}^{H \times d}$. The base policy is SmolVLA and is not updated. We train a critic Q_ϕ from rollouts generated by the base policy:

$$Q_\phi(f_o, a_{0:H-1}, e_\tau) \rightarrow \mathbb{R}, \quad (1)$$

where f_o is the policy-side observation/state feature, $a_{0:H-1}$ is a candidate action chunk, and e_τ is an optional task feature. The critic target is sparse success-to-go from real LIBERO rollouts. The critic is used only at inference time, and only through gradients with respect to the action chunk.

The deployment constraint is that the critic should consume features available to the policy at inference time. We therefore avoid privileged simulator state as critic input. Simulator success signals may be used to construct training targets, but the deployed critic path uses policy-side state features, action chunks, and task-description features.

C. SmolVLA Reverse-Time Flow Convention

The pinned SmolVLA sampler uses a reverse-time flow convention. During training, intermediate actions are constructed as

$$x_t = t\epsilon + (1-t)a, \quad v_t = \epsilon - a, \quad (2)$$

where ϵ is noise, a is the clean action chunk, and inference integrates from $t = 1$ toward $t = 0$. Given the current sample x_t and model-predicted velocity v_t , the estimated clean action is

$$\hat{a}(x_t, v_t, t) = x_t - tv_t. \quad (3)$$

This sign matters. A guidance update copied from a forward-time sampler would move the SmolVLA clean-action estimate in the wrong direction.

SmolVLA pads action chunks internally to a larger maximum action dimension, while LIBERO actions are lower-dimensional. In the implementation used for these experiments, the critic is applied only to the physical action dimensions used by LIBERO, and padded velocity dimensions are left unchanged. This prevents the critic from learning or guiding arbitrary padding coordinates.

D. Rollout Dataset and Targets

Each critic dataset is built from rollouts of the frozen SmolVLA policy. For an episode with states, policy actions, and success flags, we create overlapping chunks of horizon H . Each chunk starts at time i and uses the policy action sequence $a_{i:i+H-1}$ as the critic action input. The observation feature is the policy-preprocessed state at the start of the chunk.

The target is sparse success-to-go. Let $s_j \in \{0, 1\}$ indicate whether success has been observed at step j . For discount γ , the target at step i is

$$y_i = \begin{cases} \gamma^{j^*-i}, & j^* = \min\{j \geq i : s_j = 1\}, \\ 0, & \text{if no future success occurs.} \end{cases} \quad (4)$$

After the first success in an episode, targets are set to one. This target is simple and cheap to compute, but it is also one reason critic quality remains a bottleneck: sparse success-to-go does not directly rank all near-success action chunks.

Training and validation splits are episode-level, not random chunk-level splits. A random chunk split would leak trajectory context across train and validation because adjacent chunks from the same rollout are highly correlated. Episode-level splitting gives a stricter estimate of critic generalization.

E. Critic Architecture and Task Conditioning

The critic is a multilayer perceptron over flattened observation features, action chunks, and optional task features. The current strongest variant uses task-description features obtained from the frozen SmolVLA VLM text pathway by mean-pooling hidden states over non-padding task tokens. This is stronger than task-id conditioning because task ids are not portable across LIBERO families. The critic is trained with a mean-squared error objective:

$$\mathcal{L}(\phi) = \mathbb{E}_{(f_o, a, e_\tau, y)} \left[(Q_\phi(f_o, a, e_\tau) - y)^2 \right], \quad (5)$$

where y is sparse success-to-go.

We considered three task-conditioning choices. A task-id feature is useful for same-task tuning but does not transfer across task families. A hashed bag-of-token feature is lightweight and portable, but early experiments showed that it was too weak to produce reliable cross-task gains. The current strongest variant uses frozen SmolVLA VLM hidden-state task features. This feature keeps the critic tied to the base policy’s own language representation while avoiding a new trainable text encoder.

F. Q -Guided Flow Update

At each denoising step, we detach the base denoiser output and query the critic on the estimated clean action in (3). For an ensemble of K critics, the mean value is

$$\bar{Q}(\hat{a}) = \frac{1}{K} \sum_{k=1}^K Q_{\phi_k}(f_o, \hat{a}, e_\tau). \quad (6)$$

We compute the action gradient

$$g = \nabla_{\hat{a}} \bar{Q}(\hat{a}), \quad (7)$$

clip it to a maximum norm c , and gate it using ensemble disagreement:

$$m = \max(m_{\min}, \exp(-\alpha\sigma_Q)), \quad (8)$$

where σ_Q is the per-sample standard deviation across critic values, α is the uncertainty scale, and m_{\min} is a minimum gate. The guided velocity is

$$v_t^{\text{guided}} = v_t - \frac{m \text{clip}(g, c)}{\beta}. \quad (9)$$

The subtraction follows from the reverse-time SmolVLA convention: decreasing v_t along g increases the estimated clean action along a direction that raises critic value. The base VLA parameters remain frozen; gradients are used only with respect to the clean action estimate.

G. Runtime Procedure

The runtime procedure is summarized below. The denoiser is evaluated as usual, but the critic path temporarily enables autograd for the clean action estimate. The denoiser output is detached before critic differentiation, so the critic gradient does not backpropagate through the VLA.

- 1: **Input:** frozen policy π_θ , critics $\{Q_{\phi_k}\}_{k=1}^K$, observation features f_o , task feature e_τ , guidance parameters $(\beta, c, \alpha, m_{\min})$
- 2: Initialize x_t from the SmolVLA sampler at $t = 1$
- 3: **for** each reverse-time denoising step **do**
- 4: Compute base velocity v_t with frozen SmolVLA
- 5: Estimate clean action $\hat{a} = x_t - tv_t$
- 6: Compute $g = \nabla_{\hat{a}} K^{-1} \sum_k Q_{\phi_k}(f_o, \hat{a}, e_\tau)$
- 7: Clip g to norm c and gate it with ensemble disagreement
- 8: Set $v_t^{\text{guided}} = v_t - m \text{clip}(g, c) / \beta$
- 9: Integrate the SmolVLA sampler using v_t^{guided}
- 10: **end for**
- 11: **return** final action chunk

TABLE I
MAIN QGF EVALUATION PROTOCOLS.

Protocol	Tasks	Budget
Single-task	one LIBERO spatial task	50 episodes/seed
Spatial-only transfer	spatial validation tasks	60 episodes
Multi-family validation	spatial [5,7,8], object [6,7]	50 episodes
Multi-family held-out	spatial [6,9], object [8,9]	40 episodes

The guidance parameters control a trade-off. Smaller β produces stronger guidance, but can overrule the base policy and create regressions. Gradient clipping limits unstable critic gradients. The disagreement gate reduces guidance when ensemble members disagree, and m_{\min} keeps a small amount of guidance active even when uncertainty is high.

IV. EXPERIMENTS

A. Experimental Questions

We evaluate Guided Action Flow around three questions.

- 1) Can critic gradients improve a frozen SmolVLA policy on a task where the base policy already has nontrivial success?
- 2) Does a critic trained across a limited task family transfer, or does it produce harmful gradients on unseen tasks?
- 3) Does stronger task-description conditioning and multi-family data improve validation performance, and does that improvement survive a locked held-out test?

These questions reflect the current stage of the project. The experiments are intentionally scoped as an early arXiv study. We report the positive signal, but also include negative and weak-transfer results because they identify the main bottleneck: critic generalization.

B. Setup and Protocol

We evaluate official SmolVLA LIBERO checkpoints through the LeRobot evaluation stack [46] and real LIBERO environment rollouts, not dummy actions. The policy is kept frozen for all QGF experiments. The project targets three environment families: vanilla LIBERO, LIBERO-Plus, and LIBERO-PRO. Current QGF evidence is strongest on vanilla LIBERO; LIBERO-Plus and LIBERO-PRO are included as baseline anchors and future expansion targets.

Unless stated otherwise, QGF uses a $K = 3$ critic ensemble, gradient clipping, and an adaptive disagreement gate. The current best validation configuration uses $\beta = 2$, gradient clip norm 1.0, uncertainty scale 10, minimum gate 0.1, critic hidden dimension 768, critic depth 4, 30 critic epochs, and frozen SmolVLA VLM hidden-state task features. The base policy path is the official `lerobot/smolvla_libero` checkpoint for vanilla LIBERO experiments.

Table I summarizes the main experimental protocols. The single-task protocol tests feasibility. The spatial-only protocol tests whether a limited task-family critic transfers. The multi-family protocol is the current strongest setting and separates validation from locked held-out testing.

TABLE II
FROZEN SMOLVLA BASELINE ANCHORS.

Setting	Budget	Success
LIBERO vanilla	100 episodes	65/100 (65.0%)
LIBERO-Plus spatial subset	50 episodes	39/50 (78.0%)
LIBERO-PRO zero-shot	100 episodes	1/100 (1.0%)

C. Baseline Anchors

Table II shows practical baseline anchors for the frozen SmolVLA checkpoints before QGF is applied.

These anchors show that the frozen policy is usable on standard LIBERO and some LIBERO-Plus spatial tasks, while LIBERO-PRO is much harder under the current zero-shot setup.

The LIBERO-PRO anchor is especially important for framing. A near-zero zero-shot success rate means the base policy is not merely making small local mistakes in that setting. QGF is unlikely to repair such failures without better critic data, stronger task coverage, or a more appropriate base checkpoint. For this reason, the current QGF results should be interpreted primarily on vanilla LIBERO.

D. Single-Task QGF

The first stable positive signal uses one LIBERO spatial task and an adaptive-gated critic ensemble. This experiment asks whether the guidance path is capable of improving real closed-loop rollouts at all. Table IV reports two evaluation seed windows.

This result supports the feasibility claim: a learned critic can provide useful gradients during frozen SmolVLA inference. It is also informative because both evaluations use real environment rollouts, not action reconstruction metrics. However, earlier sweeps showed sensitivity to β , critic checkpoint selection, and gating. The same critic-guidance mechanism can create gains and regressions on different episodes. We therefore do not interpret the single-task result as evidence of broad transfer.

E. Spatial-Only Multi-Task Critic

A spatial-only multi-task critic did not generalize reliably. In a representative validation split, the frozen baseline achieved 32/60 successes, while QGF candidates achieved at most 31/60. This result is not a no-op: earlier diagnostics showed that task-conditioned guidance can change individual outcomes. The problem is that gains and regressions can cancel or tilt negative when the critic is not reliable on the evaluated tasks.

This negative result is important because it shows that adding more tasks from one family is not sufficient. A critic can still overfit, produce weak gradients, or harm unseen tasks. It also motivates the next design choices: use task-description features instead of task ids, train on multiple task families, and reduce guidance when ensemble disagreement is high.

F. Multi-Family Task-Description Critic

The strongest current variant trains on combined LIBERO spatial and object rollouts. The training set contains 500 episodes: existing LIBERO spatial tasks 0–4 plus 250 LIBERO object episodes from tasks 0–4. The object subset has 162/250 successes, and the combined training set has 332/500 successes. Table V summarizes the data and critic configuration.

Table VI reports the latest validation and locked held-out results. Hyperparameters are selected on validation tasks and then evaluated once on held-out tasks.

The validation gain is clear: QGF improves success by 10.0 percentage points on the selected validation split. The locked held-out test gain is positive but small: one additional success over 40 episodes. This pattern is the central empirical takeaway of the current project. Task-description-conditioned QGF can improve frozen VLA behavior, but critic generalization is not yet strong enough to support a broad robustness or state-of-the-art claim.

G. What the Results Show

The results support three conclusions. First, guidance is active and can affect closed-loop outcomes, as shown by the single-task gains and the changed aggregate success in the multi-family validation split. Second, task coverage matters: the spatial-only critic does not validate as a robust transfer mechanism, while the multi-family task-description critic is stronger. Third, validation performance can overstate held-out performance. The multi-family critic improves validation by 10.0 percentage points but held-out testing by only 2.5 percentage points.

The most conservative interpretation is therefore not that Guided Action Flow is a solved adaptation method. It is that frozen flow-matching VLA policies expose a useful interface for critic-guided inference, and that the quality, calibration, and task coverage of the critic determine whether this interface improves or harms behavior.

V. DISCUSSION

Guided Action Flow changes the inference-time behavior of a frozen flow-matching VLA without updating the base policy. This modularity is useful when full VLA fine-tuning is expensive or undesirable. The experiments also show why the problem is difficult. QGF can flip individual episodes from failure to success, but it can also introduce regressions. The same mechanism that makes guidance useful also makes it sensitive to critic errors. The ensemble disagreement gate reduces this risk, but it is only a first-order uncertainty heuristic.

The results suggest three practical lessons. First, the sign and time convention of the base flow sampler must be verified before applying guidance. The SmolVLA sampler uses a reverse-time convention, so the velocity update has the opposite sign from a naive forward-time expression. Second, critic train/validation splitting should be episode-level, because chunk-level leakage can overstate critic quality. Third,

TABLE III

MAIN EMPIRICAL SUMMARY. QGF IMPROVES THE FROZEN SMOLVLA POLICY IN SINGLE-TASK AND MULTI-FAMILY VALIDATION SETTINGS, WHILE THE HELD-OUT GAIN REMAINS MODEST AND THE SPATIAL-ONLY TRANSFER CRITIC IS A NEGATIVE RESULT.

Setting	Evaluation split	Baseline	QGF	Gain
Single-task QGF	seed 3000	34/50 (68.0%)	41/50 (82.0%)	+14.0 pp
Single-task QGF	seed 4000	41/50 (82.0%)	43/50 (86.0%)	+4.0 pp
Spatial-only transfer	validation	32/60 (53.3%)	$\leq 31/60 (\leq 51.7\%)$	≤ -1.7 pp
Multi-family task-description critic	validation	23/50 (46.0%)	28/50 (56.0%)	+10.0 pp
Multi-family task-description critic	held-out test	26/40 (65.0%)	27/40 (67.5%)	+2.5 pp

TABLE IV

SINGLE-TASK QGF IMPROVES THE FROZEN POLICY ON ONE LIBERO TASK.

Seed window	Baseline	QGF	Gain
3000	34/50 (68.0%)	41/50 (82.0%)	+14.0 pp
4000	41/50 (82.0%)	43/50 (86.0%)	+4.0 pp

TABLE V

MULTI-FAMILY CRITIC TRAINING DATA AND CONFIGURATION.

Item	Value
Training families	LIBERO spatial + object
Training tasks	spatial 0–4, object 0–4
Training episodes	500
Training successes	332/500 (66.4%)
Object subset successes	162/250 (64.8%)
Critic ensemble	$K = 3$
Task feature	VLM hidden state
Hidden dimension / depth	768 / 4
Epochs	30

validation-only hyperparameter selection is necessary. Retuning β or gate parameters on held-out tasks would convert the test set into another validation set and inflate the claim.

The method also illustrates a useful middle ground between pure imitation learning and full RL fine-tuning. This resembles the motivation behind residual reinforcement learning, which augments an existing controller with a learned residual rather than replacing the whole control stack [47]. In our setting, however, the residual is not an executed torque or Cartesian control correction; it is a value-gradient correction inside the action-generation trajectory of a frozen VLA sampler. The base policy remains a stable supervised VLA, while the critic supplies a task-local improvement signal at inference time. This separation is appealing for research workflows: the policy, critic, task feature encoder, and uncertainty gate can be improved independently. It also makes failure analysis more transparent. When QGF hurts performance, the likely causes can be separated into critic misranking, task-feature mismatch, OOD observations, or excessive guidance strength.

The current evidence favors uncertainty-aware guidance. A plain critic gradient can be too aggressive, especially when the critic is extrapolating. Ensemble disagreement is not a complete uncertainty estimate, but it provides a cheap signal that is available at every denoising step. Future variants can replace or augment it with task embedding distance, action-

TABLE VI

MULTI-FAMILY TASK-DESCRIPTION CRITIC RESULTS.

Split	Baseline	QGF	Gain
Validation	23/50 (46.0%)	28/50 (56.0%)	+10.0 pp
Held-out test	26/40 (65.0%)	27/40 (67.5%)	+2.5 pp

feature nearest-neighbor distance, or learned OOD detectors.

VI. LIMITATIONS

This work has several limitations. The evaluation budget is still small: the strongest multi-family held-out result contains 40 episodes. The held-out gain is positive but only 2.5 percentage points, so the paper should be read as feasibility evidence rather than a robust generalization result. Larger task sets, more seeds, and confidence intervals are needed before making stronger claims.

The critic is the main technical bottleneck. It uses compact policy-side observation features and task-description hidden states; richer visual-state features may improve value estimation. The reward target is sparse success-to-go, which is simple but may not provide enough ranking signal for action chunks that are close to success. Pairwise ranking losses or contrastive objectives over successful and failed chunks from the same task may produce more actionable gradients than pure regression.

The guidance rule is also parameter-sensitive. β , gradient clipping, ensemble size, uncertainty scale, and minimum gate all affect the balance between useful correction and harmful deviation from the base policy. The current protocol mitigates this by selecting hyperparameters on validation tasks and locking held-out tests, but it does not remove the underlying sensitivity.

Finally, LIBERO-Plus and LIBERO-PRO are not yet fully validated QGF benchmarks in this project. Current LIBERO-PRO zero-shot performance is near zero, so that setting likely requires better data coverage or a stronger base checkpoint before QGF can be meaningfully assessed. The method has not yet been evaluated on real robots, where sensor noise, latency, calibration, and recovery behavior may change the effect of action-chunk guidance.

VII. FUTURE WORK

The most direct next step is to expand critic data across more LIBERO families and evaluate with larger locked val-

idation and test budgets. A stronger critic should use better visual-state representations, not only compact policy-side state features. Another priority is to improve the critic objective. Pairwise ranking, conservative value regularization, or calibrated uncertainty losses may reduce harmful gradients on unseen tasks.

OOD-aware guidance is also important. The current gate uses ensemble value disagreement, but a deployment-oriented system should reduce or disable guidance when the observation, task embedding, or action chunk is far from the critic training distribution. Finally, real robot experiments are needed to determine whether QGF can improve a frozen VLA under execution noise and mild distribution shift outside simulation.

VIII. CONCLUSION

We presented Guided Action Flow, an inference-time Q-guided flow sampling framework for frozen flow-matching VLA policies. Applied to SmolVLA on LIBERO, the method improves single-task success and yields a clear multi-family validation gain, while locked held-out gains remain modest. The current evidence supports the core hypothesis that action-chunk critics can provide useful gradients during VLA flow inference. It also identifies critic quality, out-of-distribution detection, and validation discipline as the main challenges for making QGF-style VLA adaptation reliable.

REFERENCES

- [1] M. Shridhar, L. Manuelli, and D. Fox, "CLIPort: What and where pathways for robotic manipulation," 2021. [Online]. Available: <https://arxiv.org/abs/2109.12098>
- [2] —, "Perceiver-actor: A multi-task transformer for robotic manipulation," 2022. [Online]. Available: <https://arxiv.org/abs/2209.05451>
- [3] E. Jang, A. Irpan, M. Khansari, D. Kappler, F. Ebert, C. Lynch, S. Levine, and C. Finn, "BC-Z: Zero-shot task generalization with robotic imitation learning," 2022. [Online]. Available: <https://arxiv.org/abs/2202.02005>
- [4] A. Brohan, N. Brown, J. Carbajal, Y. Chebotar, J. Dabis, C. Finn, K. Gopalakrishnan, K. Hausman, A. Herzog, J. Hsu *et al.*, "Rt-1: Robotics transformer for real-world control at scale," 2022. [Online]. Available: <https://arxiv.org/abs/2212.06817>
- [5] A. Brohan, N. Brown, J. Carbajal, Y. Chebotar, X. Chen, K. Choromanski, T. Ding, D. Driess, A. Dubey, C. Finn *et al.*, "Rt-2: Vision-language-action models transfer web knowledge to robotic control," 2023. [Online]. Available: <https://arxiv.org/abs/2307.15818>
- [6] D. Driess, F. Xia, M. S. M. Sajjadi, C. Lynch, A. Chowdhery, B. Ichter, A. Wahid, J. Tompson, Q. Vuong, T. Yu *et al.*, "Palm-e: An embodied multimodal language model," 2023. [Online]. Available: <https://arxiv.org/abs/2303.03378>
- [7] Open X-Embodiment Collaboration *et al.*, "Open x-embodiment: Robotic learning datasets and rt-x models," 2023. [Online]. Available: <https://arxiv.org/abs/2310.08864>
- [8] Octo Model Team, D. Ghosh, H. Walke, K. Pertsch, K. Black, O. Mees, S. Dasari, H. Hejna, T. Kreiman, C. Xu *et al.*, "Octo: An open-source generalist robot policy," 2024. [Online]. Available: <https://arxiv.org/abs/2405.12213>
- [9] M. J. Kim, K. Pertsch, S. Karamcheti, T. Xiao, A. Balakrishna, S. Nair, R. Rafailov, E. Foster, G. Lam, P. Sanketi *et al.*, "Openvla: An open-source vision-language-action model," 2024. [Online]. Available: <https://arxiv.org/abs/2406.09246>
- [10] K. Black, N. Brown, D. Driess, A. Esmail, M. Equi, C. Finn, N. Fusai, L. Groom, K. Hausman, B. Ichter *et al.*, " π_0 : A vision-language-action flow model for general robot control," 2024. [Online]. Available: <https://arxiv.org/abs/2410.24164>
- [11] K. Pertsch, K. Stachowicz, B. Ichter, D. Driess, S. Nair, Q. Vuong, O. Mees, C. Finn, and S. Levine, "Fast: Efficient action tokenization for vision-language-action models," 2025. [Online]. Available: <https://arxiv.org/abs/2501.09747>
- [12] M. Shukor, D. Aubakirova, F. Capuano, P. Kooijmans, S. Palma, A. Zouitine, M. Aractingi, C. Pascal, M. Russi, A. Marafioti, S. Alibert, M. Cord, T. Wolf, and R. Cadene, "Smolvla: A vision-language-action model for affordable and efficient robotics," 2025. [Online]. Available: <https://arxiv.org/abs/2506.01844>
- [13] B. Liu, Y. Zhu, C. Gao, Y. Feng, Q. Liu, Y. Zhu, and P. Stone, "Libero: Benchmarking knowledge transfer for lifelong robot learning," 2023. [Online]. Available: <https://arxiv.org/abs/2306.03310>
- [14] S. Fei, S. Wang, J. Shi, Z. Dai, J. Cai, P. Qian, L. Ji, X. He, S. Zhang, Z. Fei, J. Fu, J. Gong, and X. Qiu, "Libero-plus: In-depth robustness analysis of vision-language-action models," 2025. [Online]. Available: <https://arxiv.org/abs/2510.13626>
- [15] X. Zhou, Y. Xu, G. Tie, Y. Chen, G. Zhang, D. Chu, P. Zhou, and L. Sun, "Libero-pro: Towards robust and fair evaluation of vision-language-action models beyond memorization," 2025. [Online]. Available: <https://arxiv.org/abs/2510.03827>
- [16] X. Tan, N. Bai, H. Gardener, Z. Zhong, L. Zhang, L. Yang, Z. Duan, M. Galeitsiwe, and Z. Tang, "Signvla: A gloss-free vision-language-action framework for real-time sign language-guided robotic manipulation," 2026. [Online]. Available: <https://arxiv.org/abs/2602.22514>
- [17] Y. Lipman, R. T. Q. Chen, H. Ben-Hamu, M. Nickel, and M. Le, "Flow matching for generative modeling," 2022. [Online]. Available: <https://arxiv.org/abs/2210.02747>
- [18] J. Ho, A. Jain, and P. Abbeel, "Denoising diffusion probabilistic models," 2020. [Online]. Available: <https://arxiv.org/abs/2006.11239>
- [19] C. Chi, Z. Xu, S. Feng, E. Cousineau, Y. Du, B. Burchfiel, R. Tedrake, and S. Song, "Diffusion policy: Visuomotor policy learning via action diffusion," 2023. [Online]. Available: <https://arxiv.org/abs/2303.04137>
- [20] P. Dhariwal and A. Nichol, "Diffusion models beat gans on image synthesis," 2021. [Online]. Available: <https://arxiv.org/abs/2105.05233>
- [21] J. Ho and T. Salimans, "Classifier-free diffusion guidance," 2022. [Online]. Available: <https://arxiv.org/abs/2207.12598>
- [22] M. Janner, Y. Du, J. B. Tenenbaum, and S. Levine, "Planning with diffusion for flexible behavior synthesis," 2022. [Online]. Available: <https://arxiv.org/abs/2205.09991>
- [23] Z. Wang, J. J. Hunt, and M. Zhou, "Diffusion policies as an expressive policy class for offline reinforcement learning," 2022. [Online]. Available: <https://arxiv.org/abs/2208.06193>
- [24] P. Hansen-Estruch, I. Kostrikov, M. Janner, J. G. Kuba, and S. Levine, "Idql: Implicit q-learning as an actor-critic method with diffusion policies," 2023. [Online]. Available: <https://arxiv.org/abs/2304.10573>
- [25] Z. Zhou, A. Peng, C. Xu, Q. Li, T. Springenberg, K. Frans, and S. Levine, "Test-time gradient guidance of flow policies in reinforcement learning," 2026. [Online]. Available: <https://arxiv.org/abs/2606.11087>
- [26] H. Zhao, Z. Tang, Z. Li, Y. Dong, Y. Si, M. Lu, and G. Panoutsos, "Real-time object detection and robotic manipulation for agriculture using a yolo-based learning approach," in *2024 IEEE International Conference on Industrial Technology (ICIT)*. IEEE, Mar 2024, pp. 1–6. [Online]. Available: <http://dx.doi.org/10.1109/ICIT58233.2024.10540740>
- [27] J. Tobin, R. Fong, A. Ray, J. Schneider, W. Zaremba, and P. Abbeel, "Domain randomization for transferring deep neural networks from simulation to the real world," 2017. [Online]. Available: <https://arxiv.org/abs/1703.06907>
- [28] X. B. Peng, M. Andrychowicz, W. Zaremba, and P. Abbeel, "Sim-to-real transfer of robotic control with dynamics randomization," 2017. [Online]. Available: <https://arxiv.org/abs/1710.06537>
- [29] A. Rajeswaran, S. Ghotra, B. Ravindran, and S. Levine, "EPOpt: Learning robust neural network policies using model ensembles," 2016. [Online]. Available: <https://arxiv.org/abs/1610.01283>
- [30] L. Pinto, J. Davidson, R. Sukthankar, and A. Gupta, "Robust adversarial reinforcement learning," 2017. [Online]. Available: <https://arxiv.org/abs/1703.02702>
- [31] C. Tessler, Y. Efroni, and S. Mannor, "Action robust reinforcement learning and applications in continuous control," 2019. [Online]. Available: <https://arxiv.org/abs/1901.09184>
- [32] E. Sariyildiz, R. Oboe, and K. Ohnishi, "Disturbance observer-based robust control and its applications: 35th anniversary overview," *IEEE Transactions on Industrial Electronics*, vol. 67, no. 3, pp. 2042–2053, 2019. [Online]. Available: <https://doi.org/10.1109/TIE.2019.2903752>

- [33] Z. Tang, J. A. Rossiter, X. Jin, B. Zhang, and G. Panoutsos, "Output tracking for uncertain time-delay systems via robust reinforcement learning control," in *2024 43rd Chinese Control Conference (CCC)*. IEEE, July 2024, pp. 2219–2226. [Online]. Available: <http://dx.doi.org/10.23919/CCC63176.2024.10662811>
- [34] Z. Tang, C. Passmore, A. I. Campbell, J. Howse, J. A. Rossiter, S. Ebbens, and G. Panoutsos, "Disturbance observer-based tracking control for roll-to-roll slot die coating systems under gap and pump rate disturbances," 2026. [Online]. Available: <https://arxiv.org/abs/2601.08488>
- [35] Z. Tang, C. Passmore, J. A. Rossiter, S. Ebbens, G. Dunderdale, and G. Panoutsos, "Disturbance observer-based optimal tracking control for slot coating process with mismatched input disturbances," in *2024 UKACC 14th International Conference on Control (CONTROL)*. IEEE, Apr 2024, pp. 55–56. [Online]. Available: <http://dx.doi.org/10.1109/CONTROL60310.2024.10531965>
- [36] Z. Tang, J. A. Rossiter, Y. Dong, and G. Panoutsos, "Reinforcement learning-based output stabilization control for nonlinear systems with generalized disturbances," in *2024 IEEE International Conference on Industrial Technology (ICIT)*. IEEE, Mar 2024, pp. 1–6. [Online]. Available: <http://dx.doi.org/10.1109/ICIT58233.2024.10540609>
- [37] Z. Tang, J. A. Rossiter, and G. Panoutsos, "A reinforcement learning-based approach for optimal output tracking in uncertain nonlinear systems with mismatched disturbances," in *2024 UKACC 14th International Conference on Control (CONTROL)*. IEEE, Apr 2024, pp. 169–174. [Online]. Available: <http://dx.doi.org/10.1109/CONTROL60310.2024.10532060>
- [38] N. Bai, C. P. Chan, Q. Yin, T. Gong, Y. Yan, and Z. Tang, "Deep reinforcement learning optimization for uncertain nonlinear systems via event-triggered robust adaptive dynamic programming," 2025. [Online]. Available: <https://arxiv.org/abs/2512.15735>
- [39] J. Hu, Z. Tang, X. Jin, B. Zhang, Y. Dong, and X. Huang, "Hierarchical testing with rabbit optimization for industrial cyber-physical systems," *IEEE Transactions on Industrial Cyber-Physical Systems*, vol. 3, pp. 472–484, 2025. [Online]. Available: <http://dx.doi.org/10.1109/TICPS.2025.3586988>
- [40] T. Gong, Y. Xu, Z. Li, Z. Tang, and Z. Ding, "Distributed time-varying optimization with inequality constraints via prescribed-time distributed average tracking," in *2025 44th Chinese Control Conference (CCC)*. IEEE, July 2025, pp. 2272–2277. [Online]. Available: <http://dx.doi.org/10.23919/CCC64809.2025.11179599>
- [41] S. Levine, A. Kumar, G. Tucker, and J. Fu, "Offline reinforcement learning: Tutorial, review, and perspectives on open problems," 2020. [Online]. Available: <https://arxiv.org/abs/2005.01643>
- [42] A. Kumar, A. Zhou, G. Tucker, and S. Levine, "Conservative q-learning for offline reinforcement learning," 2020. [Online]. Available: <https://arxiv.org/abs/2006.04779>
- [43] I. Kostrikov, A. Nair, and S. Levine, "Offline reinforcement learning with implicit q-learning," 2021. [Online]. Available: <https://arxiv.org/abs/2110.06169>
- [44] T. Yu, G. Thomas, L. Yu, S. Ermon, J. Zou, S. Levine, C. Finn, and T. Ma, "MOPO: Model-based offline policy optimization," 2020. [Online]. Available: <https://arxiv.org/abs/2005.13239>
- [45] G. An, S. Moon, J.-H. Kim, and H. O. Song, "Uncertainty-based offline reinforcement learning with diversified q-ensemble," 2021. [Online]. Available: <https://arxiv.org/abs/2110.01548>
- [46] R. Cadene, S. Alibert, A. Soare, Q. Gallouedec, A. Zouitine, S. Palma, P. Kooijmans, M. Aractingi, M. Shukor, D. Aubakirova *et al.*, "Lerobot: State-of-the-art machine learning for real-world robotics," 2024. [Online]. Available: <https://github.com/huggingface/lerobot>
- [47] T. Johannink, S. Bahl, A. Nair, J. Luo, A. Kumar, M. Loskyll, J. A. Ojea, E. Solowjow, and S. Levine, "Residual reinforcement learning for robot control," 2018. [Online]. Available: <https://arxiv.org/abs/1812.03201>